Computational Study of the Self-Initiation Mechanism in Thermal Polymerization of Methyl Acrylate

Sriraj Srinivasan,[†] Myung Won Lee,[‡] Michael C. Grady,[§] Masoud Soroush,[†] and Andrew M. Rappe*[,‡]

Department of Chemical and Biological Engineering, Drexel University, Philadelphia, Pennsylvania 19104, The Makineni Theoretical Laboratories, Department of Chemistry, University of Pennsylvania, Philadelphia, Pennsylvania 19104-6323, and DuPont Experimental Station, Wilmington, Delaware 19880

Received: April 30, 2009; Revised Manuscript Received: July 21, 2009

This computational study deals with the mechanism of spontaneous initiation in thermal polymerization of alkyl acrylates (e.g., methyl, ethyl, and *n*-butyl acrylate). The mechanism is presently still unknown. Density-functional theory (DFT) and Møller−Plesset (MP2) calculations are used to explore the Flory and Mayo mechanisms of self-initiation in methyl acrylate. On the singlet surface, a low-barrier, concerted [4 + 2] Diels−Alder mechanism for the formation of a dihydropyran adduct (**DA**) and a high-barrier nonconcerted [2 + 2] diradical (**•M$_{2s}$•**) mechanism for the formation of dimethyl cyclobutane-1,2-dicarboxylate (**DCD**) were found using B3LYP/6-31G*. Several levels of theory were used to validate the transition states, and the pathways for the **DA** and **DCD** formations on the singlet surface were determined using intrinsic reaction coordinate (IRC) calculations. On the triplet surface, a triplet diradical intermediate (**•M$_{2t}$•**) was identified that is structurally similar to **•M$_{2s}$•** but lower in energy. The spin−orbit coupling constant for crossover of the diradical from singlet to triplet surface was calculated. Monoradical generation from the two intermediates, **DA** and **•M$_{2t}$•** via hydrogen transfer to or from a third methyl acrylate was studied. It was found that generation of two monoradical species was possible from **•M$_{2t}$•** and is proposed as a likely explanation for experimentally observed spontaneous-initiation.

1. Introduction

Acrylic resins are widely used as primary binders in coatings formulations for the automobile industry.[1] Due to stringent environment regulations to reduce volatile organic content[2] (VOC), resins with lower solvent content, lower average molecular weight, and higher functionality have replaced previous formulations. A resin with higher functionality has more dead-polymer chains that are capable of undergoing further reactions. High-temperature (above 373 K) polymerization of acrylates had to be used to produce low-average-molecular-weight resins in place of traditional low-temperature polymerization.[3−5] Although trace quantities of initiators have been reported by Chiefari et al. to be sufficient to initiate polymerization,[3] thermal initiators are fairly expensive, and residual initiators are known to cause undesirable coloration in resins.[6] While claims have been made that spontaneous thermal polymerization in alkyl acrylates was not possible,[7] Grady et al.[8] reported sustained, reproducible, spontaneous, thermal polymerization of alkyl acrylates in the absence of any known extrinsic initiators at temperatures above 373 K. It has been speculated that trace quantities of inherent hydroperoxide impurities in the monomers may be initiating polymerization, but electrospray ionization-Fourier transform mass spectrometry (ESI-FTMS) profiles indicated the lack of such end group structures.[9] Rantow et al.[10] probed the initiation step using nuclear magnetic resonance spectroscopy (NMR) and macroscopic mechanistic modeling, but the results were inconclusive. Due to the large size of the system of interest, density-functional-theory (DFT)[11]-based methods are attractive alternatives to wave-function-based quantum chemical methods[12] to predict the initiating species and mechanism of initiation. Although DFT-based methods are not nearly as accurate in predicting barriers[13] as the highest-level quantum chemical techniques are, the efficiency of DFT permits analysis of complex multiatom systems like the acrylate dimers studied here. The use of modern hybrid exchange-correlation and decent basis sets has been shown to yield reasonable agreement with experimental values for reactions (i.e., initiation, propagation, chain transfer) occurring in free radical polymerization.[12,14] In addition, once potential energy surfaces are explored approximately with DFT, higher-level approaches are valuable for local analysis of important molecular structures.

The self-initiation of styrene has been extensively studied, and the mechanisms proposed by Flory[15] and Mayo[16] serve as important prototypes. Mayo[16] proposed that two molecules of styrene undergo a [4 + 2] cycloaddition reaction to form a Diels−Alder intermediate which is often denoted as **AH** because it can lose a hydrogen to a third monomer to produce a pair of monoradicals that initiate polymerization. According to the Flory[15] mechanism, two monomers undergo [2 + 2] cycloaddition reaction to form a cyclobutane dimer (**CBD**), and this ring can open to form a diradical (**•M$_{2s}$•**), which can abstract a hydrogen atom from a third monomer to form monoradicals that initiate polymerization. Khuong et al.[17] pointed out that self-initiation could possess aspects of both the Flory and Mayo mechanisms. They proposed a stepwise diradical mechanism in place of a concerted pathway for formation of **AH**, which can then undergo hydrogen transfer to initiate polymerization. Numerous experimental studies[18−20] have validated Mayo's

* Corresponding author. E-mail: rappe@sas.upenn.edu.
[†] Drexel University.
[‡] University of Pennsylvania.
[§] DuPont Experimental Station.

10.1021/jp904036k CCC: $40.75
Published on Web 09/11/2009

mechanism by detecting the presence of a Diels−Alder (**AH**) intermediate in thermal polymerization of styrene. DFT calculations using B3LYP/6-31G* and BPW91/6-31G* levels of theory confirmed **AH** to be the key intermediate in styrene polymerization and hydrogen transfer from **AH** as the monoradical generating reaction.[17]

Pryor and Lasswell[21] suggested that Flory's mechanism can be extended to various monomers, e.g., methyl methacrylate (MMA), with a (**$^{\bullet}M_{2t}^{\bullet}$**) triplet diradical species initiating polymerization for monomers other than styrene. It has become clear that the insights from styrene do not necessarily apply to acrylates or methacrylates. Stickler and Meyerhoff[22] agreed, suggesting that Mayo's mechanism does not lead to spontaneous polymerization of MMA, because the **AH** intermediate is incapable of undergoing homolysis and generating monoradicals. They also reported that the activation energy for dimer formation via a Flory-type **$^{\bullet}M_{2s}^{\bullet}$** (146 kJ mol^{-1}) was comparable with that of the initiation step. This supported the conclusion that diradicals probably initiate polymerization, but no concrete evidence of whether it was in the singlet or triplet state was reported.

Salem and Rowland[23] proposed that the bifunctional behavior of diradicals allows free mixing of closely lying singlet and triplet states, which under favorable conditions can produce radiationless crossover from singlet to triplet ($S_0 \rightarrow T_1$). This process is known as intersystem crossing (ISC), and the most common mechanism through which it can occur is known as spin-orbit coupling (SOC). Previous studies[24] on hydrocarbon diradicals and oxygen-containing diradicals have shown that SOC effectively describes the mixing of singlet and triplet states, so SOC is the main mechanism that governs intersystem crossing. Significant intersystem crossing can be facilitated by a dense continuum of vibrational states, as found in relatively large molecules such as benzene.[25,26] Smaller diradicals can undergo intersystem crossing via collision with solvent or inert gases.[27,28] The singlet−triplet energy difference in homosymmetric diradicals such as ethylene has been shown to be generally small (35.6 kJ mol^{-1}) in comparison to heterosymmetric diradicals such as linear methylene (129.7 kJ mol^{-1}).[29,30]

Solution-phase free radical polymerization can be affected by solvent molecules in various ways that can lead to a significant difference in the calculated and experimental rate constants.[31] Due to its high dielectric constant, a polar solvent can stabilize transition state structures and reduce reaction barriers. Solvents can affect reactions, viz., propagation, chain transfer via specific interactions such as hydrogen bonding or complex formation and via bulk diffusion effects. In addition, the solvent affects the calculated entropy of activation and consequently rate constants of bimolecular reactions. The effect of polar interactions can be treated with continuum models.[32] However, these models fail to account for entropy differences or the effect of direct solvent interactions. Quantum modeling of solutes and solvent molecules has been reported to be computationally infeasible in polymerization systems.[33] No simplified model currently exists to reduce the difference between gas and solution phase rate constants. Calculations using a continuum model to study solvent effects on propagation in free radical polymerization of acrylic acid have shown that introduction of the toluene solvent field into the calculations had little effect on the activation energy and transition state structures estimated via gas-phase simulations.[34] Furthermore, experiments using xylene and other inert solvents show no effect on the initiation reaction in spontaneous thermal polymerization of methyl acrylate (MA).[8] Therefore, in this study, gas-phase calculations are performed, and the rigid rotor harmonic oscillator approximation (RRHO) is used to calculate the thermodynamics and kinetics of the reactions.

Treatment of internal rotation in small and large molecules has been extensively studied in the last 60 years.[35,36] Pitzer[35] used the one-dimensional rigid rotor model to describe anharmonic motions associated with low-frequency vibrational modes in equilibrium and transition state geometries. In recent years, the one-dimensional hindered rotor model[36] has been used to compute the vibrational partition function for free-radical polymerization of ethylene, vinyl chloride, acrylonitrile, and acrylate monomers, and it has shown good agreement between calculated and experimental propagation rate constants. The predicted enthalpies and activation energies have been shown to be insensitive to the choice of rotor model. While the harmonic oscillator approximation tends to overestimate frequency factors and rate constants, it is computationally less demanding, and it has been found to be highly accurate in comparison to the hindered rotor model in a few large molecules. Rate constants comparable to experiment were predicted in self-initiation in thermal polymerization of styrene[17] using B3LYP/6-31G*, without applying the hindered rotor model. In the present study, no internal rotation treatment has been applied. The calculated rate constants may be overestimated somewhat due to neglect of internal rotation, but this effect is not likely to be significant, and the reported barriers and activation energies are expected to be adequately accurate.

In this paper, DFT[11] is used to explore the Flory and Mayo mechanisms of self-initiation for methyl acrylate (Figure 1). The formation of key intermediates on the singlet and triplet surfaces is studied. An energy map of the singlet surface is constructed to describe the pathways for the formation of the **DA** and **DCD** using B3LYP/6-31G*.[37,38] Validation of the transition states is performed with different levels of theory. The triplet energy surface is calculated. Spin-orbit coupling constants[39] for singlet−triplet crossover are estimated using MCSCF/6-31G*. Monoradical generation via hydrogen transfer from **DA** and triplet diradical is studied. Energy barriers for the dimer and monoradical formation are calculated. The paper is organized as follows. Section 2 describes computational methods used in the study. Section 3 presents and discusses the computational results. Finally, concluding remarks are given in section 4.

2. Computational Methods

All theoretical calculations in this work were performed using GAMESS.[40] DFT calculations on the singlet and triplet surfaces were performed using restricted open-shell and unrestricted wave functions, respectively. B3LYP/6-31G* was chosen as the level of theory to construct the potential energy surface profiles and estimate transition states due to its successful use in the study of free radical polymerization of alkenes and self-initiation of styrene.[12,14,17] No DFT study has been conducted for self-initiation in MMA or any alkyl acrylate previously. The molecular geometries of reactants, products, and transition states were optimized on the singlet and triplet surfaces. Vibrational frequency calculations were performed to characterize reactants and transition states. Intrinsic reaction coordinate calculations were performed in the forward and reverse directions to determine minimum-energy pathways. Assessment of the transition states and energy barriers was performed with various basis sets and with DFT and MP2: B3LYP/6-31G**, B3LYP/6-311G*, B3LYP/6-31G(2df,p), MP2/6-31G**, MP2/6-31G*, and MP2/6-311G*. Spin−orbit coupling calculations were carried out using MCSCF/6-31G*. Reported energies (relative to the energy of the reactant) were calculated using a rigid rotor

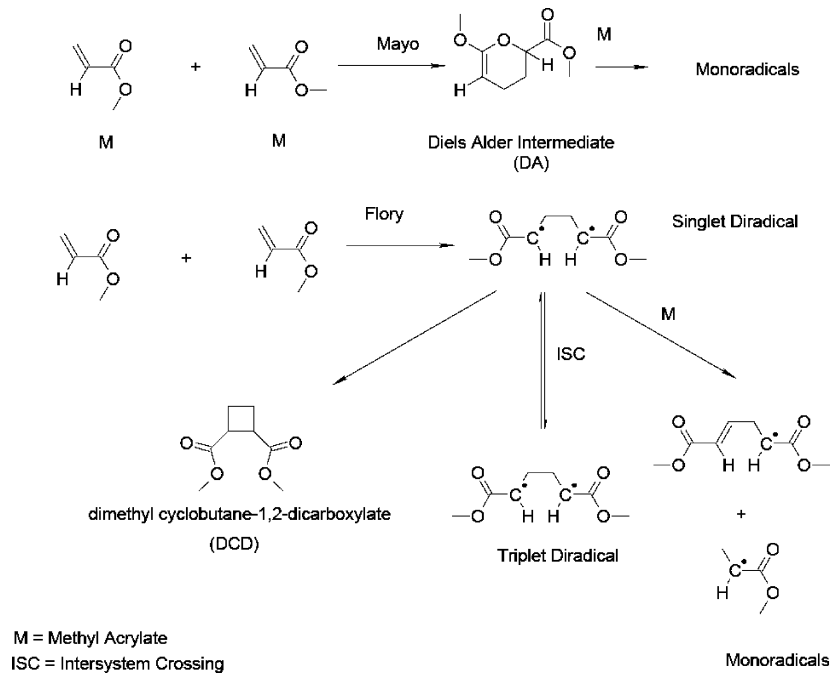

Figure 1. Flory and Mayo mechanisms of self-initiation for methyl acrylate.

harmonic oscillator approximation (RRHO).[41] Scaling factors to calculate activation entropy, temperature correction, and zero point vibrational energy at different levels of theory were taken from the National Institute of Standards and Technology (NIST) Computational Chemistry Comparison and Benchmark DataBase.[42] Rate constants were calculated using transition state theory,[43] and the Wigner tunneling correction[44] was used. All calculations were performed in the gas phase.[11,15,17]

3. Results and Discussion

3.1. Singlet Energy Surface. The singlet potential energy surface profile was constructed by constraining two internuclear distances, 1.45 Å ≤ r(C6−C13) ≤ 2.4 Å and 1.6 Å ≤ r(C1−C14) ≤ 3.4 Å, as shown in Figure 2. The numbers inserted in the plot point to the potential energies of some of the key chemical structures drawn below the plot. Multiple peaks and valleys representing saddle points and minima on the reaction pathways were verified by calculating Hessian matrices. All minima have positive eigenvalues, and all saddle points have one negative eigenvalue.

3.1.1. Diels−Alder Intermediate Formation. The thermal cycloaddition [4 + 2] reaction was studied between the conjugated diene C6═C1−C2═O3 of one methyl acrylate monomer and the dienophile C13═C14 of a second. Concerted reaction pathways were found that agreed with orbital symmetry rules.[45] The exo, **2**, and endo, **3**, transition states were identified, and the energy of the endo transition state was predicted to be ≈2.1 kJ mol^{-1} lower than the exo transition state. This energy difference is so small that both products can be produced concurrently. However, the formation of one product over another may depend upon steric interactions and electrostatic repulsions between the parts of the **DA**. *Meta* orientation **DA** dimers (Chart 1) were obtained as the final products from the calculations, and a negligible difference (<1 kJ/mol) in energies exists between the *meta* and *para* orientation **DA**. This suggests that the initial orientation of the reactants can influence which product is formed.

The geometry of the exo transition state, **2**, is r(C6−C13) = 1.767 Å, r(C1−O3) = 2.21 Å, and ϕ(C1−C6−C13−C14) = −66.2°, and the endo transition state, **3**, is r(C6−C13) = 1.773 Å, r(C1−O3) = 2.24 Å, and ϕ(C1−C6−C13−C14) = 62.9°. The single imaginary frequency calculated for the exo and endo transition states is 356.6i and 360.1i cm^{-1}, respectively. No internal rotation treatment was performed for low-frequency modes that exist in the transition state geometries. The energy barrier for the formation of the exo product, **4**, is 117.1 kJ mol^{-1} (zero point energy corrected) above that of the reactant, which is 2.1 kJ mol^{-1} higher than that of the endo product, **5**. In the reaction, one of these products (**4** or **5**) will be preferred as a thermodynamic product and the other as a kinetic product. The lowest energy product is the thermodynamic product, which is found by comparing the molecular energies of the exo and endo products, respectively. The energy of the endo **DA**, **5**, is higher than the exo **DA**, **4**, by ≈2.9 kJ mol^{-1}. Therefore, the exo product is the thermodynamic product. The kinetic product is identified by comparing energies of the endo and exo **DA** transition states; the endo transition state has a lower energy and is the kinetic product. The kinetic product is favored when the temperature of the reaction is insufficient to overcome the energy barrier and the thermodynamic product is favored at high enough temperatures when sufficient energy is available to overcome the barrier. In spontaneous high-temperature polymerization of methyl acrylate, the formation of exo **DA** is predicted to be significant. Results from intrinsic reaction coordinate (IRC) calculations from the transition state, **2**, in the forward and reverse directions are shown in Figure 3. In each direction, 250 points were calculated.

We modeled the exo transition state, **2**, with different basis sets and with DFT and MP2, as shown in Table 1. Calculations show that B3LYP and MP2 yield transition state geometries and energy barriers that are significantly different, as given in Table 1. B3LYP/6-31G (2df, p), was selected because it has been shown to be a reliable level of theory in G3[46,47] and G4[48] to calculate geometries and transition states. In order to obtain an accurate thermochemical estimate for the reactions under study, calculations were performed using G4 theory. We encountered computational difficulties while using higher levels of theory, e.g., coupled cluster or MP4 methods with a large

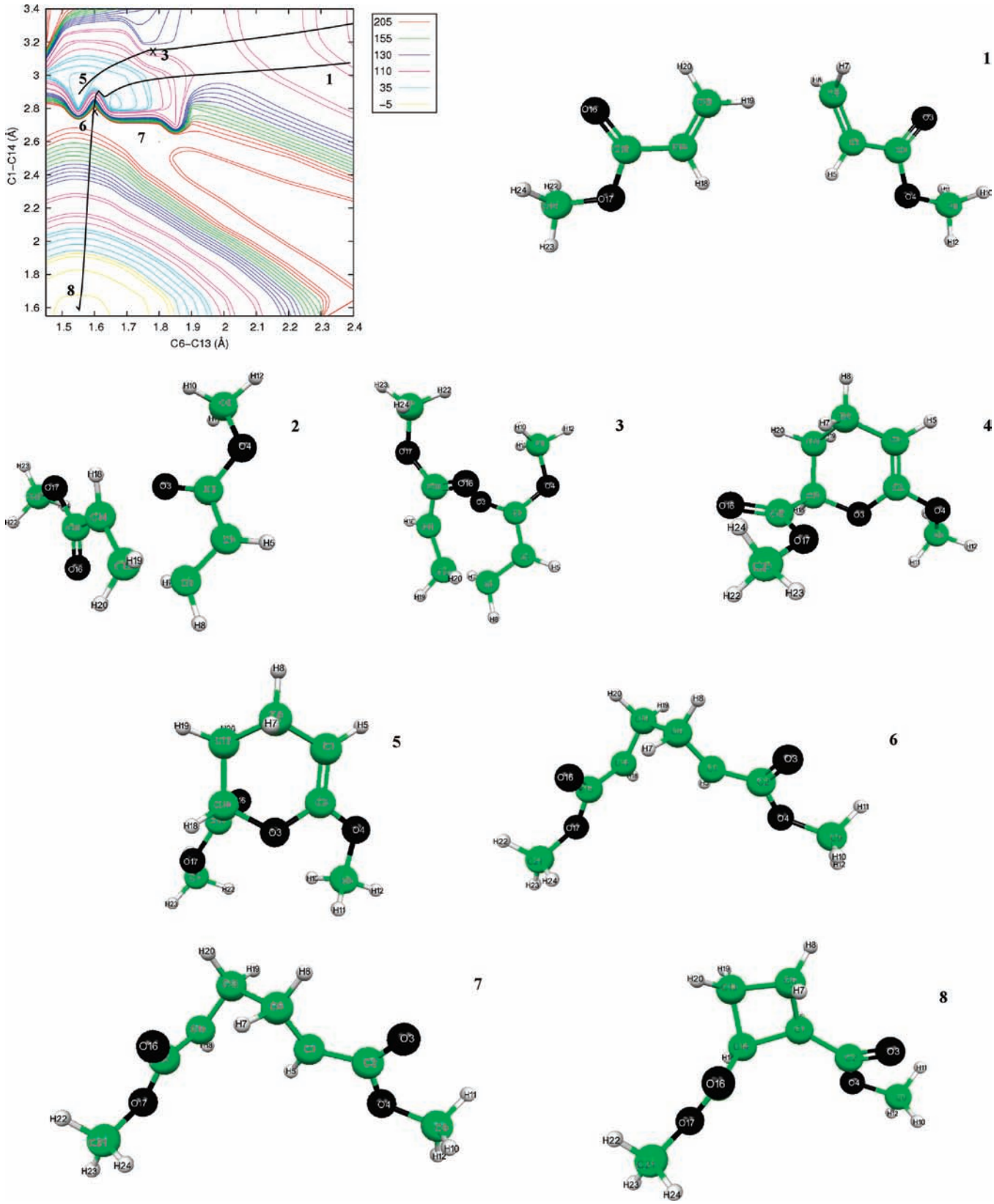

Figure 2. Contour map of the singlet potential energy surface. r(C1−C14) vs r(C6−C13). All energies are relative to that of the reactant in kJ mol^{-1}. All bond lengths in Å. Color scheme (highest to lowest energy): red, green, blue, magenta, cyan, yellow. The points on the low-energy pathways are connected by black lines. **1**, methyl acrylate (MA) monomers; **2**, exo transition state (**TS$_{exo}$**); **3**, endo transition state (**TS$_{endo}$**); **4**, exo product (**DA$_{exo}$**); **5**, endo product (**DA$_{endo}$**); **6**, singlet diradical transition state (**$^{\bullet}$M$_{2s}^{\bullet}$**); **7**, diradical on flat region on singlet surface; **8**, dimethyl cyclobutane-1,2-dicarboxylate (**DCD**).

basis set, due to the large size of the methyl acrylate system. In view of these, we believe that the true value of activation energy, enthalpy, frequency factor, and rate constant for **DA** formation lies within the range of values shown in Table 1, and these values serve as a reasonable *a priori* prediction for experimental verification.

CHART 1: *Para* and *Meta* Isomers of DA

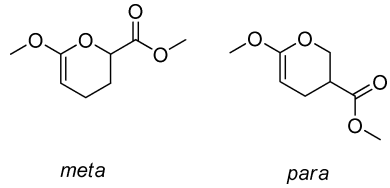

*3.1.2. Dimethyl Cyclobutane-1,2-dicarboxylate (***DCD***) Formation.* We found a nonconcerted [2 + 2] thermal cycloaddition reaction to occur between C1═C6 and C13═C14 atoms to form **DCD**. Figure 2 shows that the formation of **DCD** is via a singlet gauche conformation diradical transition state (**6**). The extensive flat region on the singlet surface (**7**) suggests that the system (diradical) may be induced to spend a longer time exploring the surface before ring closure. The geometry of the calculated diradical transition state (**6**) is r(C6−C13) = 1.597 Å, r(C1−C14) = 2.788 Å, and ϕ(C1−C6−C13−C14) = 57.6°.

Figure 3 depicts the reaction pathway for the formation of **DCD**, **8**, from **6**. The flat region on the singlet surface can act like an intermediate, as reported by Hoffmann et al.[49] for the tetramethylene diradical who termed this geometry a "twixtyl". It is fundamentally similar to the stereorandom one-step diradical decay process proposed by Dervan et al.[50] in diazene-derived tetramethylene, but it is different from the two independent stereorandom steps model of Doubleday Jr.[51,52] for cyclobutane-derived tetramethylene. We found that the transformation from the methyl acrylate reactants to **DCD** is highly stereospecific, which is in good agreement with the Woodward−Hoffmann rules for electrocyclic reactions.[45] **DCD**, **8**, is of *cis* orientation, and is produced from **6**, with the same stereochemistry (Scheme 1). Furthermore, the *trans* diradical that is required to produce *trans* **DCD**, can be produced by internal rotation of **6** (Scheme 1). The diradical, **6**, is formed stereospecifically and then is scrambled via internal rotation to form the *trans* diradical. The scrambling stops with the formation of *trans* **DCD**, and the stereochemistry from the *trans* diradical is transferred intact to the product. This suggests that the stereorandomness in methyl acrylate is built after formation of a diradical via internal rotation. The diradical, **6**, in one step decays to yield **DCD** (Scheme 1), which agrees with the model of Dervar et al.[50] The two-step stereorandom model[51,52] involves shared transition states, and stereorandomness is built into the formation and decay of the diradical. The absence of this model in our calculations can be attributed to the generalized notion that the stereochemistry of the forming diradical is dependent on the precursor (methyl acrylate) and as dynamical treatment is required to predict the two-step model.[52] Experiments have not shown **DCD** formation in spontaneous thermal polymerization of methyl acrylate.[8] High monomer conversion[8] (≥80%) indicates the preference to form polymers in comparison to dimers. It may be possible that trace concentrations of **DCD** do form as in spontaneous polymerization of MMA[22] but have been unmeasured. It is highly probable that the singlet diradical undergoes intersystem crossing to form a triplet diradical, which can act as an intermediate for generating initiating monoradical species.[22,53] The transition state and energy barriers obtained from the B3LYP/6-31G* were compared with those calculated using other levels of theory, as given in Table 2. We found MP2 to show lower barriers and no significant difference in the bond lengths of the predicted geometries in comparison to B3LYP.

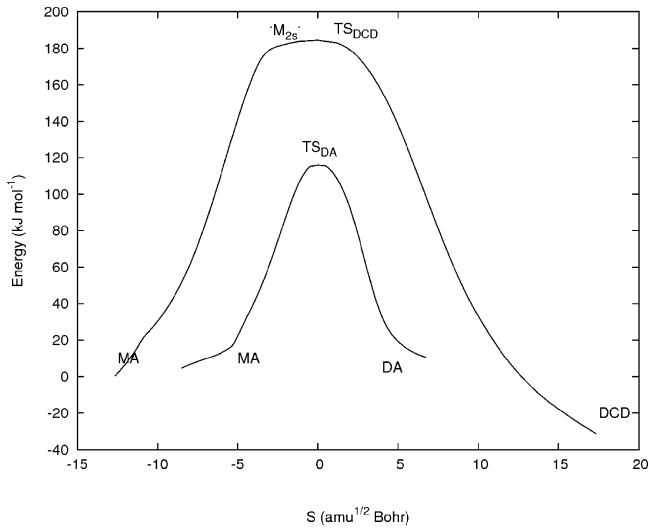

Figure 3. Intrinsic reaction coordinate path to **DA** and **DCD** dimer formation in methyl acrylate. The flat potential energy surface has diradical structures. The energy is relative to that of the reactant.

3.2. Triplet Energy Surface and Spin-Orbit Coupling. The energy contour map of the triplet surface is shown in Figure 4. The triplet and singlet surfaces are dramatically different. We found a diradical intermediate (**9**) with a bond length between C6 and C13 r(C6−C13) = 1.552 Å, no real bond between C1 and C14 r(C1−C14) = 3.021 Å, and a dihedral angle ϕ(C1−C6−C13−C14) = 62.2°, as shown in Figure 4. All frequencies were positive, confirming that this structure is a local minimum. The energy of the triplet diradical intermediate is 113 kJ/mol above that of the reactant (zero point energy corrected).

We found that there is a strong structural similarity between the singlet gauche diradical transition state, **6** (r(C6−C13) = 1.597 Å, ϕ(C1−C6−C13−C14) = 57.6°) and the triplet diradical intermediate, **9** (r(C6−C13) = 1.552 Å, ϕ(C1−C6−C13−C14) = 62.2°). The differences in bond lengths and angles are ≈0.045 Å and ≤5°, respectively. We estimated the spin−orbit coupling constant using MCSCF (6,6)/6-31G* for the singlet−triplet crossover to be A = 1.94 cm^{-1}. The energy difference between the ground-state singlet diradical and the lowest-energy triplet level (ΔE_{S-T}) is 78 kJ mol^{-1}, which is comparable to ΔE_{S-T} = 70 kJ mol^{-1} predicted using B3LYP/6-31G*. According to Salem and Rowland,[23] even if a vibronic degeneracy exists between the singlet and triplet diradical, a large density of states in the reaction manifold is required for intersystem crossing. Methyl acrylate is a fairly large molecule, and the diradical has ionic character in the singlet state (μ = 2.91 D), and both are favorable conditions for intersystem crossing. Solvent-induced intersystem crossing that can lead to formation of triplet diradical initiating species has been shown to occur in spontaneous thermal polymerization of MMA with halogenated solvents at high temperatures.[53] It is speculated that the high temperatures (above ca. 120 °C) at which spontaneous thermal initiation in methyl acrylate polymerization has been reported[8−10] may induce sufficient collisions between the diradical and solvent to ensure the occurrence of the intersystem crossing.

3.3. Monoradical Generation. Monoradical formation in thermal polymerization of styrene has been proposed to occur through the molecular-assisted homolysis mechanism,[16−20] which involves hydrogen transfer from the Diels−Alder intermediate to a third monomer to generate two monoradicals. We tested this mechanism by performing a hydrogen transfer reaction from

TABLE 1: Bond Length, Activation Energy (E_a), Enthalpy ($\Delta H^{\ddagger}_{298}$), and Free Energy ($\Delta G^{\ddagger}_{298}$) in kJ mol^{-1}, Frequency Factor (A) and Rate Constant for exo DA Formation (k_{DA}) in M^{-1} s^{-1} at 298 K Using Different Levels of Theory[a]

level of theory	r(C14−O3), Å	r(C6−C13), Å	E_a	$\Delta H^{\ddagger}_{298}$	$\Delta G^{\ddagger}_{298}$	$\log_e A$	k_{DA}
B3LYP/6-31G*	2.243	1.773	123.37	118.41	177.80	8.67	1.41×10^{-18}
B3LYP 6-31G**	2.236	1.772	125.63	120.67	176.99	9.91	1.96×10^{-18}
B3LYP 6-311G*	2.218	1.758	135.62	130.66	187.98	9.50	2.32×10^{-20}
B3LYP 6-31G(2df,p)	2.199	1.767	132.97	128.01	184.73	9.74	8.63×10^{-20}
MP2 6-31G*	2.009	1.665	93.9	89	152.34	7.07	4.07×10^{-14}
MP2 6-31G**	2.009	1.665	91.96	87	150.37	7.06	9.05×10^{-14}
MP2 6-311G*	1.992	1.677	109.35	104.39	167.28	7.25	9.83×10^{-17}

[a] The reported energies are zero point vibrational energy (ZPVE) corrected.

TABLE 2: Bond Length, Activation Energy (E_a), Enthalpy ($\Delta H^{\ddagger}_{298}$), and Free Energy ($\Delta G^{\ddagger}_{298}$) in kJ mol^{-1}, Frequency Factor (A), and Rate Constant for DCD Formation (k_{DCD}) in M^{-1} s^{-1} at 298 K Using Different Levels of Theory[a]

level of theory	r(C1−C14), Å	r(C6−C13), Å	E_a	$\Delta H^{\ddagger}_{298}$	$\Delta G^{\ddagger}_{298}$	$\log_e A$	k_{DCD}
B3LYP 6-31G*	2.788	1.597	191.15	186.20	242.98	9.72	5.37×10^{-30}
B3LYP 6-31G**	2.783	1.597	191.08	186.12	241.64	10.23	9.21×10^{-30}
B3LYP 6-311G*	2.779	1.593	199.08	194.12	248.94	10.51	4.85×10^{-31}
B3LYP 6-31G(2df,p)	2.740	1.596	223.18	218.22	269.46	11.95	1.23×10^{-34}
MP2 6-31G*	2.816	1.554	145.27	140.32	197.10	9.71	5.86×10^{-22}
MP2 6-31G**	2.821	1.554	148.43	143.48	200.14	9.76	1.72×10^{-22}
MP2 6-311G*	2.808	1.560	145.98	141.02	198.23	9.55	3.73×10^{-22}

[a] The reported energies are zero point vibrational enery (ZPVE) corrected.

SCHEME 1: Stereorandom One-Step Diradical Mechanism

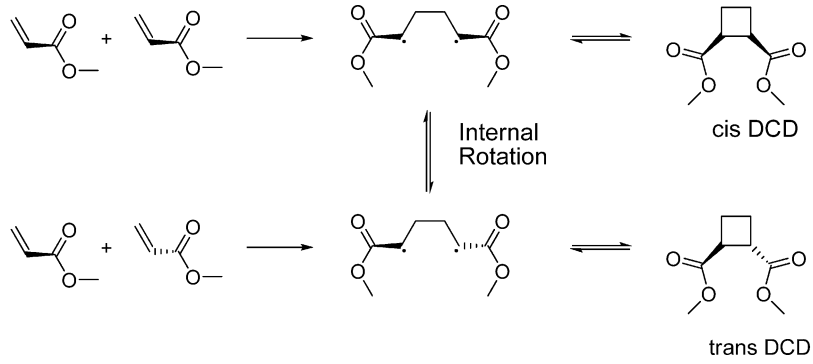

the **DA** intermediate using B3LYP/6-31G* on the singlet surface. The r(C1−H5) and r(H5−C25) bond lengths were constrained such that 1.19 Å ≤ r(C1−H5) ≤ 1.59 Å and 1.19 Å ≤ r(H5−C25) ≤ 1.59 Å during geometry optimization. We found no hydrogen transfer from the **DA** intermediate to generate monoradicals. The Diels−Alder intermediate formed in styrene after hydrogen cleavage has been shown to aromatize in order to stabilize the monoradical,[17] but this was found to be absent in the methyl acrylate **DA**. Since MA has an oxygen heteroatom, we tested hydrogen abstraction from the monomer by oxygen by constraining bond lengths, r(C1−H5) and r(H5−O25); the pathway showed high-energy monoradicals and almost no barrier to back reaction, so that hydrogen transfer would not occur. We conclude that hydrogen transfer from **DA** in methyl acrylate polymerization is not possible for monoradical generation to initiate polymerization, which supports a similar finding of Stickler and Meyerhoff[22] in thermal polymerization of MMA.

We found that the singlet diradical undergoes ring closure before hydrogen transfer, which suggests that monoradical generation from the triplet may be the most favorable path. Hydrogen transfer from $^{\bullet}\mathbf{M_{2t}}^{\bullet}$ to a third monomer (Scheme 2) was studied using B3LYP/6-31G* by constraining r(C6−H7) and r(H7−C25) such that 1.19 Å ≤ r(C6−H7) ≤ 1.59 Å and 1.19 Å ≤ r(H7−C25) ≤ 1.59 Å. Hydrogen abstraction by $^{\bullet}\mathbf{M_{2t}}^{\bullet}$ from a third monomer was studied constraining 1.19 Å ≤ r(C26−H25) ≤ 1.59 Å and 1.19 Å ≤ r(H25−C14) ≤ 1.59 Å (Scheme 2). Transition state geometries for hydrogen transfer, **10**, and abstraction, **11**, as shown in Figure 5, are r(C25−H7) = 1.39 Å and r(C6−H7) = 1.40 Å and r(C26−H25) = 1.48 Å and r(C14−H25) = 1.25 Å, respectively. It can be seen from Table 3 that the hydrogen transfer reaction has a lower activation energy (E_a) than the hydrogen abstraction reaction by approximately 15 kJ mol^{-1}. The Wigner tunneling correction model[44] was applied to calculate rate constants of transfer and abstraction reactions. If better agreement with experiments is necessary, sophisticated methods such as small curvature approximation[54] can be used. Higher rate constants for hydrogen transfer to monomer further suggest that it may be favored over hydrogen abstraction from monomer. We rationalize that higher activation energy of abstraction reaction is a consequence of the lesser ability of methine (CH) to release the hydrogen atom in comparison to methylene (CH_2). It can be seen from Scheme 2 that the loss of hydrogen atom from the methine group generates a radical species that is structurally unstable that may be incapable of initiating polymerization. These suggest that monoradical generation in self-initiation of methyl acrylate occurs via hydrogen transfer from $^{\bullet}\mathbf{M_{2t}}^{\bullet}$ to monomer.

4. Concluding Remarks

The self-initiating mechanisms of Flory and Mayo were extensively examined to understand spontaneous thermal initia-

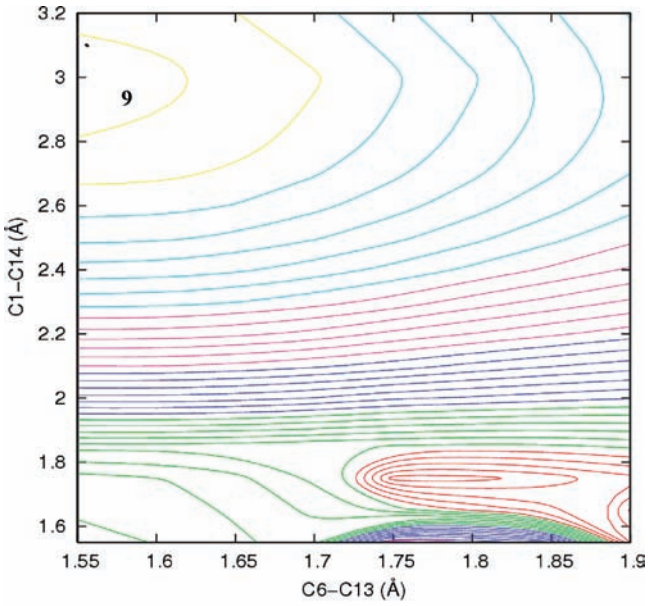

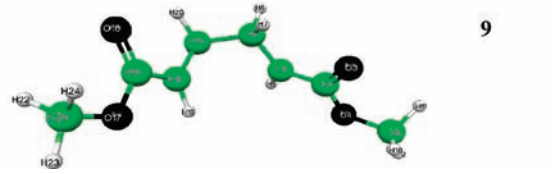

Figure 4. Contour map of the triplet potential energy surface. r(C1−C14) vs r(C6−C13). All energies are relative to the singlet reactant in kJ mol^{-1}. All bond lengths in Å. Color nomenclature (highest to lowest energy): red, green, blue, magenta, cyan, yellow. **9**: triplet diradical intermediate.

SCHEME 2: Hydrogen Abstraction and Transfer Reactions via Triplet Diradical

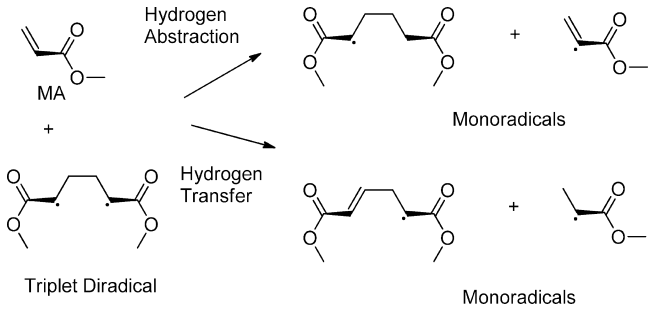

tion in high-temperature polymerization of methyl acrylate using B3LYP/6-31G*. Pathways for endo and exo **DA** were found. The transition state for the endo **DA** was observed to be slightly lower (≈2.1 kJ mol^{-1}) than that of the exo **DA**. The nonconcerted singlet diradical pathway for formation of **DCD** was found with an energy barrier 70 kJ mol^{-1} higher than that of the endo **DA**. Validation of the transition states and energy barriers was carried out using several levels of theory. MP2 was found to predict similar transition geometries but lower energy barriers than B3LYP. A key intermediate, the triplet diradical, which forms via intersystem crossing from the singlet diradical was found. The spin orbit coupling constant for this crossover has been predicted to be a low value, $A = 1.94$ cm^{-1}. The monoradical generation was found not to occur by hydrogen transfer from **DA**. Hydrogen transfer from triplet diradical to monomer was found to cause monoradical generation. In summary, the evidence points to the mechanism of spontaneous

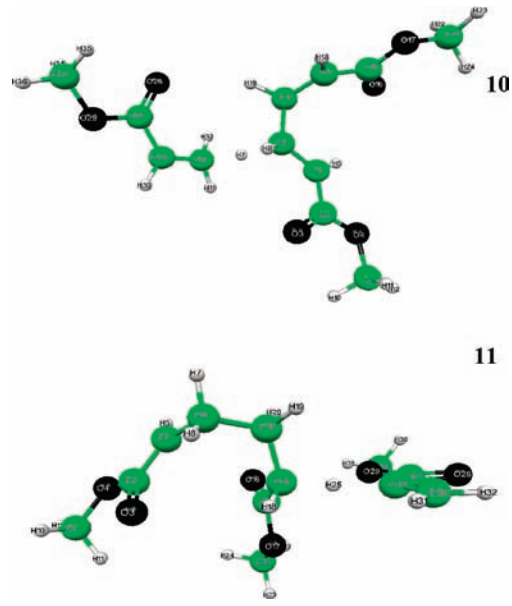

Figure 5. Transition state geometry for formation of monoradicals from the triplet diradical.

TABLE 3: Activation Energy (E_a), Enthalpy ($\Delta H^{\ddagger}_{298}$), and Free Energy ($\Delta G^{\ddagger}_{298}$) in kJ mol^{-1}, Frequency Factor (A), and Rate Constant for Monoradical Formation via Hydrogen Abstraction (k_{HA}) and Hydrogen Transfer (k_{TR}) in M^{-1} s^{-1}[a]

T, K	E_a	$\Delta H^{\ddagger}$	$\Delta G^{\ddagger}$	log$_e$ A	k^c without tunneling	Wigner[b]	k^c with tunneling
Hydrogen Transfer from $^{\bullet}M_{2t}{}^{\bullet}$ to MA							
298	81.14	76.19	115.96	16.58	9.67×10^{-8}	4.81	4.65×10^{-7}
373	83.74	77.54	125.79	17.51	7.59×10^{-5}	3.43	2.61×10^{-4}
413	85.16	78.3	130.92	17.95	1.06×10^{-3}	2.98	3.16×10^{-3}
Hydrogen Abstraction by $^{\bullet}M_{2t}{}^{\bullet}$ from MA							
298	96.97	92.01	134.08	15.65	6.45×10^{-11}	2.67	1.73×10^{-10}
373	99.44	93.24	144.50	16.54	1.81×10^{-7}	2.07	3.76×10^{-7}
413	100.79	93.59	147.25	16.95	4.12×10^{-6}	1.87	7.72×10^{-6}

[a] The reported barriers are zero point vibrational energy (ZPVE) corrected. [b] Wigner tunneling correction.[44] [c] Rate constant from transition state theory.[43]

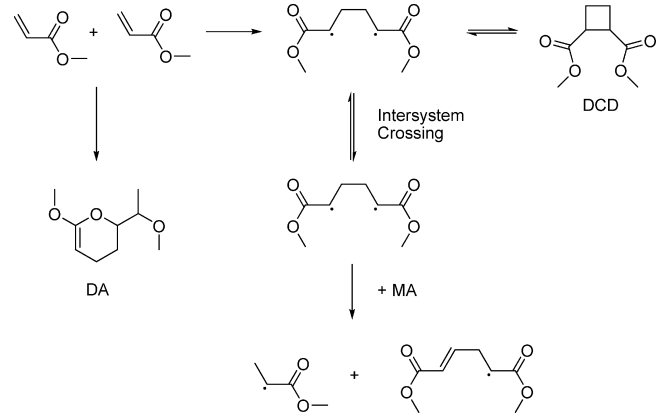

Figure 6. Proposed mechanism of self-initiation in thermal polymerization of methyl acrylate.

thermal initiation of methyl acrylate being via diradicals that are in the triplet state (as shown in Figure 6). Therefore, this study supports the claim of Pryor and Lasswell[17] that the Flory diradical mechanism can explain spontaneous polymerization of other molecules beyond styrene.

Acknowledgment. This study was supported in part by DuPont Marshall Laboratory. S.S. and M.S. acknowledge the National Science Foundation (NSF) through grant CBET-0651706. A.M.R. was supported by the US Department of Energy through grant DE-FG02-07ER15920, and M.W.L. by the US Air Force Office of Scientific Research, under grant FA9550-07-1-0397. Computational support was provided by the High-Performance Computing Modernization Office of the US Department of Defense.

Supporting Information Available: Cartesian coordinates and total energies of the stationary points and total energies of the geometries at fixed grid points of singlet and triplet potential energy surfaces. This material is available free of charge via the Internet at http://pubs.acs.org.

References and Notes

(1) Adamsons, K.; Blackman, G.; Gregorovich, B.; Lin, L.; Matheson, R. *Prog. Org. Coat.* **1998**, *34*, 64.
(2) VOC's Directive, EU Committee of the American Chamber of Commerce in Belgium, ASBL/VZw, Brussels, July 8, 1996.
(3) Chiefari, J.; Jeffery, J.; Mayadunne, R. T. A.; Moad, G.; Rizzardo, E.; Thang, S. H. *Macromolecules* **1999**, *32*, 7700–7702.
(4) Buback, M.; Klingbeil, S.; Sandmann, J.; Sderra, M. B.; Vögele, H. P.; Wackerbarth, H.; Wittkowski, L. Z. *Z. Phys. Chem.* **1999**, *210*, 199–221.
(5) Grady, M. C.; Simonsick, W. J.; Hutchinson, R. A. *Macromol. Symp.* **2002**, *182*, 149–168.
(6) Peter, A. C.; Moskal, M. G. http://www.arkema-inc.com/literature/pdf/304.pdf. Arkema Inc.: King of Prussia, PA.
(7) Walling, C.; Briggs, E. R.; Mayo, F. R. *J. Am. Chem. Soc.* **1946**, *68*, 1145–1149.
(8) Grady, M. C.; Quan, C.; Soroush, M. Patent Application Number 60/484,393, filed on July 2, 2003, status: pending.
(9) Quan, C.; Soroush, M.; Grady, M. C.; Hansen, J. E.; Simonsick, W. J. *Macromolecules* **2005**, *38*, 7619–7628.
(10) Rantow, F. S.; Soroush, M.; Grady, M. C.; Kalfas, G. A. *Polymer* **2006**, *47*, 1423–1435.
(11) Hohenberg, P.; Kohn, W. *Phys. Rev.* **1964**, *136*, B864–871.
(12) Wong, M. W.; Radom, L. *J. Phys. Chem.* **1995**, *99*, 8582–8588.
(13) Cohen, A. J.; Mori-Sánchez, P.; Yang, W. *Science* **2008**, *321*, 792–794.
(14) Van Speybroeck, V.; Van Cauter, K.; Coussens, B.; Waroquier, M. *ChemPhysChem* **2005**, *6*, 180–189.
(15) Flory, P. J. *J. Am. Chem. Soc.* **1937**, *59*, 241–253.
(16) Mayo, F. R. *J. Am. Chem. Soc.* **1953**, *75*, 6133–6142.
(17) Khuong, K. S.; Jones, W. H.; Pryor, W. A.; Houk, K. N. *J. Am. Chem. Soc.* **2005**, *127*, 1265–1277.
(18) Hiatt, R. R.; Bartlett, P. D. *J. Am. Chem. Soc.* **1959**, *81*, 1149–1154.
(19) Mayo, F. R. *J. Am. Chem. Soc.* **1968**, *90*, 1289–1295.
(20) Buzanowski, W. C.; Graham, J. D.; Priddy, D. B.; Shero, E. *Polymer* **1992**, *33*, 3055–3059.
(21) Pryor, W. A.; Lasswell, L. D. *Adv. Free-Radical Chem.* **1975**, *5*, 27–99.
(22) Lingnau, J.; Stickler, M.; Meyerhoff, G. *Eur. Polym. J.* **1980**, *16*, 785–791.
(23) Salem, L.; Rowland, C. *Angew. Chem. Int. Ed.* **1972**, *11*, 92–111.
(24) Minaev, B. F.; Agren, H. *THEOCHEM* **1998**, *434*, 193–206.
(25) Robinson, G. W. *J. Chem. Phys.* **1967**, *47*, 1967–1979.
(26) Anderson, L. G.; Paramenter, C. S. *J. Chem. Phys.* **1970**, *52*, 466–468.
(27) Eder, T. W.; Carr, R. W. *J. Chem. Phys.* **1970**, *53*, 2258–2266.
(28) Kropp, P. J. *J. Am. Chem. Soc.* **1969**, *91*, 5783–5791.
(29) Dunning, T. H.; Hunt, W. J.; Goddard, W. A., III. *Chem. Phys. Lett.* **1969**, *4*, 147–150.
(30) Harrison, J. F.; Allen, L. C. *J. Am. Chem. Soc.* **1969**, *91*, 807–823.
(31) Coote, M. *Encycl. Polym. Sci. Technol.* **2006**, 1–57.
(32) Pleigo Jr, J. R.; Riveros, J. M. *J. Phys. Chem. A* **2001**, *105*, 7241–7247.
(33) Truhlar, D. G.; Garrett, B. C.; Klippenstein, S. J. *J. Phys. Chem.* **1996**, *100*, 12771–12800.
(34) Thickett, S. C.; Gilbert, R. G. *Polymer* **2004**, *45*, 6993–6999.
(35) Pitzer, K. S.; Gwinn, W. D. *J. Chem. Phys.* **1942**, *10*, 428–440. Truhlar, D. G. *J. Comput. Chem.* **1991**, *12*, 266–27. Ayala, P. Y.; Schlegel, H. B. *J. Chem. Phys.* **1998**, *108*, 2314–2325. Van Speybroeck, V.; Van Neck, D.; Waroquier, M.; Wauters, S.; Saeys, M.; Marin, G. B. *J. Phys. Chem. A* **2000**, *104*, 10939–10950.
(36) Pfaendtner, J.; Yu, X.; Broadbelt, L. J. *Theor. Chem. Acc.* **2007**, *118*, 881–898, and references therein.
(37) Becke, A. D. *Phys. Rev. A* **1988**, *38*, 3098–3100.
(38) Lee, C.; Yang, W.; Parr, R. G. *Phys. Rev. B* **1988**, *37*, 785–789.
(39) Fedorov, D. G.; Koseki, S.; Schmidt, M. W.; Gordon, M. S. *Int. Rev. Phys. Chem.* **2003**, *22*, 551–592.
(40) Schmidt, M. W.; Baldridge, K. K.; Boatz, J. A.; Elbert, S. T.; Gordon, M. S.; Jensen, J. H.; Koseki, S.; Matsunaga, N.; Nguyen, K. A.; Su, S. J.; Windus, T. L.; Dupuis, M.; Montgomery, J. A. *J. Comput. Chem.* **1993**, *14*, 1347.
(41) Irikura, K. K. *THERMO.PL*; National Institute of Standards and Technology: 2002.
(42) http://cccbdb.nist.gov.
(43) Eyring, H. *J. Chem. Phys.* **1935**, *3*, 107–115.
(44) Wigner, E. P. *Z. Phys. Chem.* **1932**, *B19*, 203–216.
(45) Woodward, R. B.; Hoffmann, R. *J. Am. Chem. Soc.* **1965**, *87*, 395–397.
(46) Baboul, A. G.; Curtiss, L. A.; Redfern, P. C. *J. Chem. Phys.* **1999**, *110*, 7650–7657.
(47) Curtiss, L. A.; Raghavachari, K. *Theor. Chem. Acc.* **2002**, *108*, 61–70.
(48) Curtiss, L. A.; Redfern, P. C.; Raghavachari, K. *J. Chem. Phys.* **2007**, *126*, 084108−1−084108−12.
(49) Hoffmann, R.; Swaminathan, S.; Odell, B. G.; Gleiter, R. *J. Am. Chem. Soc.* **1970**, *92*, 7091–7097.
(50) Dervan, P.; Santilli, D. J. *J. Am. Chem. Soc.* **1980**, *102*, 3863–3870.
(51) Doubleday, C., Jr.; Camp, R. N.; King, H. F.; McIver, J. W., Jr.; Mullally, D.; Page, M. *J. Am. Chem. Soc.* **1984**, *106*, 447–448.
(52) Doubleday, C., Jr. *J. Am. Chem. Soc.* **1993**, *115*, 11968–11983.
(53) Lingnau, J.; Meyehoff, G. *Makromol. Chem.* **1984**, *185*, 587–600.
(54) Skodje, R. T.; Truhlar, D. G.; Garrett, B. C. *J. Phys. Chem.* **1981**, *85*, 3019–3023.

JP904036K